# Dense 3D pressure discomfort threshold (PDT) map of the human head, face and neck
## A new method for mapping human sensitivity

Smulders, M.; van Dijk, L.N.M.; Song, Y.; Vink, P.; Huysmans, T.

**DOI**
10.1016/j.apergo.2022.103919

**Publication date**
2023

**Document Version**
Final published version

**Published in**
Applied Ergonomics

Applied Ergonomics 107 (2023) 103919

Contents lists available at ScienceDirect

Applied Ergonomics

journal homepage: www.elsevier.com/locate/apergo

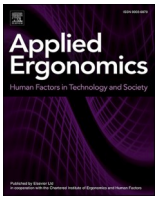

# Dense 3D pressure discomfort threshold (PDT) map of the human head, face and neck: A new method for mapping human sensitivity

M. Smulders [a,*], L.N.M. van Dijk [b], Y. Song [a], P. Vink [a], T. Huysmans [a,c]

[a] Faculty of Industrial Design Engineering, Delft University of Technology, Landbergstraat 15, 2628CE, Delft, the Netherlands
[b] Crescent Medical B.V., Vlamingstraat 72A, 2611KZ, Delft, the Netherlands
[c] Imec-Vision Lab, Department of Physics, University of Antwerp, Universiteitsplein 1, B-2610, Antwerp, Belgium

ARTICLE INFO

*Keywords:*
Comfort
Digital human modelling
3D scanning
Wearables
Pressure ulcers

ABSTRACT

When designing wearables that interface with the human head, face and neck, designers and engineers consider human senses, ergonomics and comfort. A dense 3D pressure discomfort threshold map could be helpful, but does not exist yet. Differences in pressure discomfort threshold for areas of the head, neck and face were recorded, to create a 3D pressure discomfort threshold map.

Between 126 and 146 landmarks were placed on the left side of the head, face and neck of twenty-eight healthy participants (gender balanced). The positions of the landmarks were specified using an EEG 10–20 system-based landmark-grid on the head and a self-developed grid on the face and neck. A 3D scan was made to capture the head geometry and landmark coordinates. In a randomised order, pressure was applied on each landmark with a force gauge until the participant indicated experiencing discomfort. By interpolating all collected pressure discomfort thresholds based on their corresponding 3D coordinates, a dense 3D pressure discomfort threshold map was made.

A relatively low-pressure discomfort threshold was found in areas around the nose, neck front, mouth, chin-jaw, cheek and cheekbone, possibly due to the proximate or direct location of nerves, blood veins and soft (muscular) tissue. Medium pressure discomfort was found in the neck back, forehead and temple regions. High pressure discomfort threshold was found in the back of the head and scalp, where skin is relatively thin and closely supported by bone, making these regions interesting for mounting or resting head, face and neck related equipment upon.

## 1. Introduction

When designing products that humans touch, wear and interact with, designers and engineers always consider the human senses and ergonomics, as contact pressure of a product to the human skin has an influence on the comfort experience of use (Fenko et al., 2010; Goossens, 2009; Mergl, 2006; Vink and Hallbeck, 2012; Zenk et al., 2006). Too high contact pressure can lead to discomfort or even pain (Shah et al., 2017). Insight on pressure sensitivity, expressed as pressure discomfort threshold (PDT) (Buso and Shitoot, 2019; Fischer, 1986; Shah and Luximon, 2021; Vink and Lips, 2017; Xiong et al., 2011), of different areas could lead to new design requirements and/or recommendations. A 3D PDT map could provide a theoretical base for adapting the interface softness, location and surface area between user and head-, eye-, ear- and face-wearables and equipment for medical, aeronautical, maritime, consumer and defence applications. Such applications could be: helmets, (medical) head mounted cameras and magnification, glasses, marine-, Augmented Reality- (AR), and Virtual Reality- (VR) goggles (Lee, Kim, Molenbroek, Goossens and You, 2019), headphones, headsets, hearing aids, medical-, aeronautic-, and industrial masks and respirators (Lee et al., 2019; Zhuang and Bradtmiller, 2005), sleeping pillows and headrests (Franz et al., 2012). To design more comfortable products, designers and engineers might need more detailed information on head, face, and neck sensitivity.

Many studies have been conducted on finding PDT, and/or pressure pain threshold (PPT) of the head. Antonaci, Bovim, Fasano, Bonamico, and Shen (1992) investigated pain of pressure on the frontal, parietal, occipital, temporal, zygomatic and posterior-parotid regions of the head (n=40) based on 11 symmetrical landmarks on each side of the head,

* Corresponding author.
*E-mail addresses:* m.smulders@tudelft.nl, info@maximsmulders.com (M. Smulders), y.song@tudelft.nl (Y. Song), p.vink@tudelft.nl (P. Vink), t.huysmans@tudelft.nl (T. Huysmans).

https://doi.org/10.1016/j.apergo.2022.103919
Received 5 June 2022; Received in revised form 22 September 2022; Accepted 10 October 2022
Available online 11 November 2022

**Abbreviations**

| | |
|---|---|
| CAD | Computer-aided design: the use of computers to aid in the creation, modification, analysis, or optimisation of a design |
| EEG | Electroencephalography: an electrodiagnostic technique for evaluating and recording the electrical activity produced by the brain |
| PDT | Pressure Discomfort Threshold: tissue sensitivity for pressure, determined by the amount of pressure over a given area in which a steadily increasing nonpainful pressure stimulus turns into a discomfortable pressure sensation |
| PPT | Pressure Pain Threshold: deep muscular tissue sensitivity for pressure, determined by the amount of pressure over a given area in which a steadily increasing nonpainful pressure stimulus turns into a painful pressure sensation (O'Hora et al., n.d.) |

where Brough and Konz (1992) investigated discomfort of pressure on the frontal, parietal and temporal regions of the head (n=30) based on 48 landmarks (24 left, 24 right). Hung and Samman (2009) investigated static light touch, 2-point static, and pain detection thresholds in *"normal young Chinese individuals"* (n=100) on the infraorbital, upper- and lower-labial, and chin on the left and right sides of the head, based on 8 landmarks. Shah and Luximon (2021) investigated pressure sensitivity of the human head, face and partly the neck in Chinese adults (n=218) based on 76 landmarks (38 left, 38 right).

Though researchers paid considerable efforts on head sensitivity, most of these studies were limited in sample size, sex balance, landmark density, testing region and/or availability of data. A higher landmark density could provide designers and engineers a more precise PDT map that could enable them to design more comfortable product-user interfaces. Also, most of these studies did not cover, or only covered a limited section of the neck, where this could be crucial in designing the interfaces between human and products like neck braces, headrests and helmets.

The aim of this study is to create a high-density 3D PDT map of the head, face and neck for the better understanding of the pressure sensitivity of humans, as well as facilitating designers and engineers in designing products that interface with these regions.

## 2. Participants, materials and method

PDT was measured in 28 healthy participants on 126 to 146 landmarks (135 on average) on the left side of the head, face and neck, as previous studies found no significant differences between the left and right side of the head (Antonaci et al., 1992; Brough and Konz, 1992; Posnick et al., 1990; Shah and Luximon, 2021). Since previous studies indicate repeated trials give similar results (Antonaci et al., 1992; Posnick et al., 1990; Shah and Luximon, 2021), and in order to maintain the feasibility of the study with the available resources, no repeated trials were conducted. The landmarks' 3D coordinates of each participant were captured by means of 3D scanning and mapped to a reference head. The PDT values of all participants were bilaterally mirrored and interpolated to create a complete 3D PDT map of the human head, face and neck.

### 2.1. Participants

14 female and 14 male (14 Dutch, 6 Chinese, 3 Italian, 1 Costa Rican, 1 Thai, 1 American, 1 Belgian and 1 Danish-German) adults with no history of a stroke, epilepsy, seizure, stenosis, and/or injuries or physical complaints at the face, neck and/or head in the past six months participated in this study (see Table 1). Participants with tape and/or glue allergies were excluded from the experiment, as sticker landmarks were used on the skin.

### 2.2. Apparatus

Pressure gauges have been used in the past to measure PPT (e.g. Antonaci et al. (1992); Fischer (1986); Shah and Luximon (2021)) and PDT (e.g. Broekhuizen et al. (2019); Buso and Shitoot (2019); Shah and Luximon (2021); Vink and Lips (2017)). In this study, a Mecmesin AFG 500N pressure gauge was used to apply pressure stimuli perpendicular to the skin on landmarked locations (see Fig. 1), capturing the PDT in Newtons.

Where Vink and Lips (2017) used a ø20 mm probe tip for probing the buttocks and back, Fischer (1987) and Broekhuizen et al. (2019) used a 1 $cm^2$ probe, and Antonaci et al. (1992), Brough and Konz (1992) and Buso and Shitoot (2019) used a ø10 mm probe tip for probing the head, feet and other body parts. As a ø10 mm probe is small enough to capture small facial features (e.g. nose tip) for a high-density measurement, a 3D printed ø10 mm PLA pressure gauge probe with rounded edges (3 mm fillet) was made for this study (see Fig. 1). Rounded edges were used to prevent high pressure at the surface edge (Buso and Shitoot, 2019; Fransson-Hall and Kilbom, 1993). PLA (Polylactic acid) was chosen for its biocompatibility (Ramot et al., 2016) and low thermal conductivity regarding metal probes, as a cold sensation might influence thermal comfort of the user (Parsons, 2003).

Ø12 mm stickers were used as landmarks. A hair cap was used to hygienically cover the hair, in order to place a head-cap with an EEG 10–20 landmarks grid (Jasper, 1958) (see Fig. 1) to landmark the positions on the head. An Artec Eva 3D scanner was used to capture the 3D geometry of the head and landmark coordinates. A Canon EOS 60D camera was used to make reference photos of the landmarks.

A massage seat was used to support the head (preventing movement and muscle activation caused by giving counter-pressure) while probing PDT.

### 2.3. Procedure

Written consent was obtained prior to the experiment. Stature height and weight were measured, and age, gender and ethnicity/nationality were noted.

**Table 1**
Characteristics of participants.

| | | Mean | SD |
|---|---|---|---|
| *Female (n=14)* | *Age [Years]* | 35.4 | 14.4 |
| | *Stature [cm]* | 168.5 | 5.0 |
| | *Weight [Kg]* | 59.2 | 7.8 |
| *Male (n=14)* | *Age [Years]* | 31.5 | 11.9 |
| | *Stature [cm]* | 179.1 | 9.5 |
| | *Weight [Kg]* | 73.6 | 7.9 |

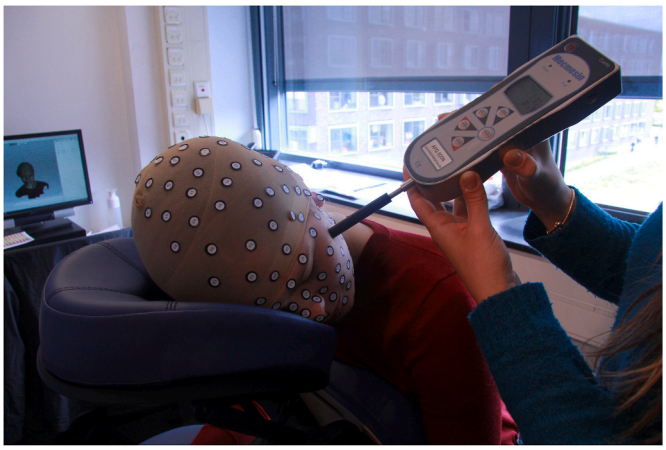

**Fig. 1.** Mecmesin AFG 500N pressure gauge with 3D printed PLA Ø10 mm tip, and participant with EEG 10–20 landmark grid headcap and landmark stickers on the face, head and neck. Researcher gradually increasing pressure on a landmark with pressure gauge until the participant indicates the PDT has been reached.

#### 2.3.1. Landmark placement and capture

Participants were asked to clean their face and neck with hypoallergenic cleaning wipes for better landmark sticker adhesion. Researchers cleaned their hands with disinfectant alcohol gel.

Participants with long hair were asked to make a bun to the right side of the head, next to the ear, to minimise influence of the hair on the 3D scan (in order to scan close to the actual scalp) and PDT measurements.

Participants then sat down, where two researchers placed a clean hair cap over the hair and pushed hair underneath as much as possible. Next, the head-cap with the EEG 10–20 landmark grid was placed on top. 126 to 146 landmarks (135 on average) were placed by two researchers on the face and neck (see Fig. 2). Some of these landmarks were placed based on clearly identifiable anatomical landmarks (e.g. tragus, lateralis ad alare, philtrum, protuberantia mentalis, and commissura labiorum, as indicated on a reference model), where others were at intermediate locations (see Fig. 2). The goal was to gain a compact spread over the entire head, face and neck, with a distance of 2–3 cm between landmarks. Some participants with broad necks got an extra row of landmark-stickers in the back of the neck and some got extra landmarks around the ear to cover some 'blind spots'.

With an Artec Eva 3D scanner, the geometry of the head, face and neck, and the landmark coordinates were captured. Thereafter reference photos of the landmarks where made.

#### 2.3.2. Sensitivity experiment procedure

All landmark-points were divided over four zones, to limit the number of postural changes, which were passed in order. For pressure on the head (zone 1) and the back of the neck (zone 4), participants were asked to take position A (see Fig. 3): with the face down on the head support. For pressure on the face (zone 2), participants were asked to take position B (see Fig. 3): with the face sideways on the headrest, respectively. For pressure on the lower chin and neck front (zone 3), participants were asked to take position C (see Fig. 3): sitting upright, respectively.

The experiment was conducted in two sessions: the first was for priming, where participants got acquainted with the procedure with a limited number of landmarks being pressed. Thereafter participants

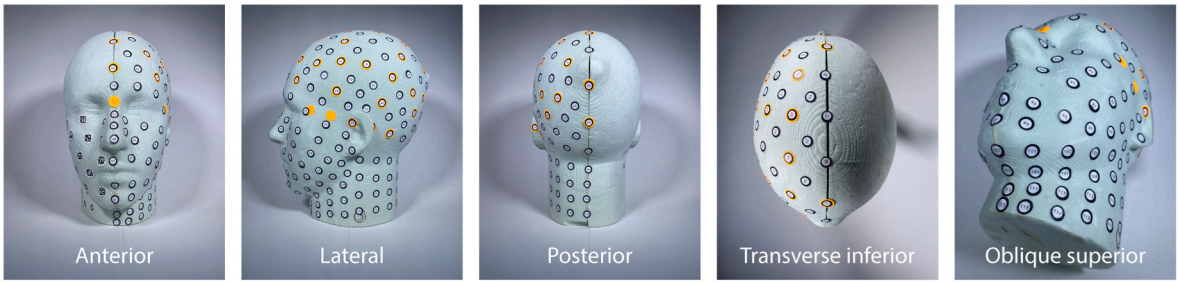


**Fig. 2.** Landmark location reference model (black landmarks only).

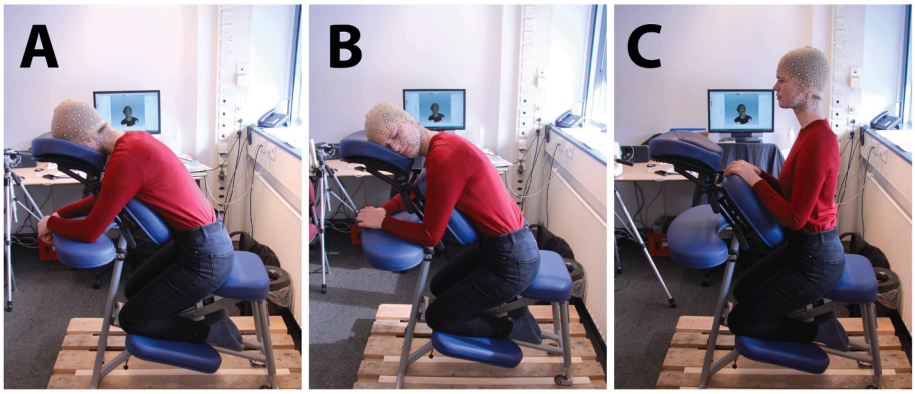


**Fig. 3.** Position A: participant in massage seat, face down. Position B: participant in massage seat, face sideways. Position C: participant in massage seat, head up.

were asked to stand up and have a 5-min break, to limit the impact of the priming on the second session. In the second session, all landmarks in each zone were probed in a randomised order and data was collected. For each landmark, a researcher gradually applied pressure on the centre of the landmark with the probe of the pressure gauge along the normal direction of the face/head/neck in this region (see Fig. 1). Participants were instructed to slap with their hand on the arm rest when applied pressure was considered uncomfortable. Pressure was then released by the researcher and the recorded maximum force was documented.

### 2.4. Measures

#### 2.4.1. 3D scan processing

In Artec Studio 14, 3D scans of each participant were pre-processed (e.g. fill holes), aligned and merged as a 3D textured mesh, which was exported in OBJ format.

#### 2.4.2. 3D landmark allocation and numbering

A Python program was developed to allocate the correct landmark ID number to each landmark. Landmark IDs were visually identified based on the allocated number in the scan, or when illegible, the reference photos were used.

#### 2.4.3. Intra-individual pressure distribution processing

To compare relative PDT differences between participants, the PDT's were normalised per participant by expressing the PDT as a percentage of the mean of the top 5% PDT of the individual participant. Mean5% MaxPDT was chosen to limit the effect of outliers on the normalisation.

#### 2.4.4. Mean 3D head model

To create the PDT map, a mean head model was made from the 3D scans of all participants. The 3D scan of each participant was rigidly aligned with a standard head mesh template in R3DS Wrap 3.4, based on predefined landmarks on the glabella, nose apex, between the alar nasal sulcus-nasolabial sulcus, philtrum, ear lobule and protuberantia occipitalis externa. Next, the mesh template was wrapped on the 3D scan while matching the predefined landmarks (i.e. elastically deform the mesh template to match the shape of the 3D scan), which utilises a variant of the non-rigid iterative closest points algorithm (Dyke et al., 2020). The results were visually checked and interactively adjusted where needed. This process was iterated over all 28 3D scans.

Based on these 28 3D scans, a mean head model was made using a Python script (Huysmans et al., 2020), where all meshes were aligned (Gower, 1975). The mean coordinates were calculated for each vertex (point), from which the mean head mesh was created. The complete process ensures a point-to-point correspondence between the mean model and each 3D scan.

#### 2.4.5. Bilaterally symmetric modelling

Using the one-to-one correspondence between the mean model and each participant's 3D scan, landmark locations of each 3D scan were mapped onto the average head model. Note that, due to the manual landmak placement, the landmark locations can slightly differ between participants, and thus also end up at slightly different locations on the average head, as shown in Fig. 4.

Bilateral symmetry was accomplished by utilizing a left-right correspondence on the average head, which was obtained by wrapping a left-right mirrored version of the average head to the original average head. By averaging the vertex coordinates of two head models, an average and symmetric head model was obtained.

In creating the symmetric average model, clipping of the surface to a region of interest (ROI) was needed. To this end the ROI was limited to those parts of the model where for 90% of the participants there was at least 1 landmark within a 30 mm range.

#### 2.4.6. 3D pressure discomfort threshold map

PDT values between landmarks were obtained from a smooth interpolation of the values at landmark locations to the rest of the average head model, by solving for a solution with a vanishing Laplacian at all vertices (method B from Oostendorp et al. (1989)). The resulting symmetric PDT maps, defined on the symmetric average head model, allowed to calculate summary statistics of PDT over the full set of participants or for gender-specific sub-groups (e.g. see Figs. 5 and 6). The same approach was used to create maps of normalised PDT values (Mean5%MaxPDT).

#### 2.4.7. Statistical analysis

Where previous studies like Shah and Luximon (2021) statistically analyse individual landmarks, this study uses a method with anatomical independent landmarking in order to achieve greater landmark density. This method however does not allow for landmark based analysis, as placed landmarks do not always correspond between participants within this study and previous studies. Therefore, zones are drawn to conduct statistical analysis and compare results with previous studies. Zones *scalp*, *forehead*, *temple*, *back head, nose*, *cheekbone*, *cheek*, *mouth*, *jaw-chin*, *neck front*, and *neck back* are based on zones of potential interest for different wearables, anatomical features, underlying tissue, landmark locations and observed PDT transitions (see Fig. 4).

A Mann-Whitney-Wilcoxon test (two-tailed) was used for comparing gender differences and a Kruskal-Wallis test for identifying difference in median PDT across zones ($p<.05$). A Dunn's Post-hoc (pairwise) tests was used to identify differences per combination of zones, which was compensated for multiple comparisons by controlling False Discovery Rate through the Benjamini-Hochberg procedure.

Analysis of gender difference was conducted based on both absolute- and normalised PDT data (Mean5%MaxPDT). All other statistical analysis were conducted based on absolute PDT values only (thus no interpolated nor mirrored data were used).

## 3. Results

### 3.1. Average PDT map

In Fig. 4 the landmark dense 3D PDT map is shown. The mean and standard deviation (SD) 3D PDT maps of all participants, males and females are shown in Figs. 5 and 6. The standard deviation is more prevalent at the *forehead*, *scalp*, *back head* and *back neck*.

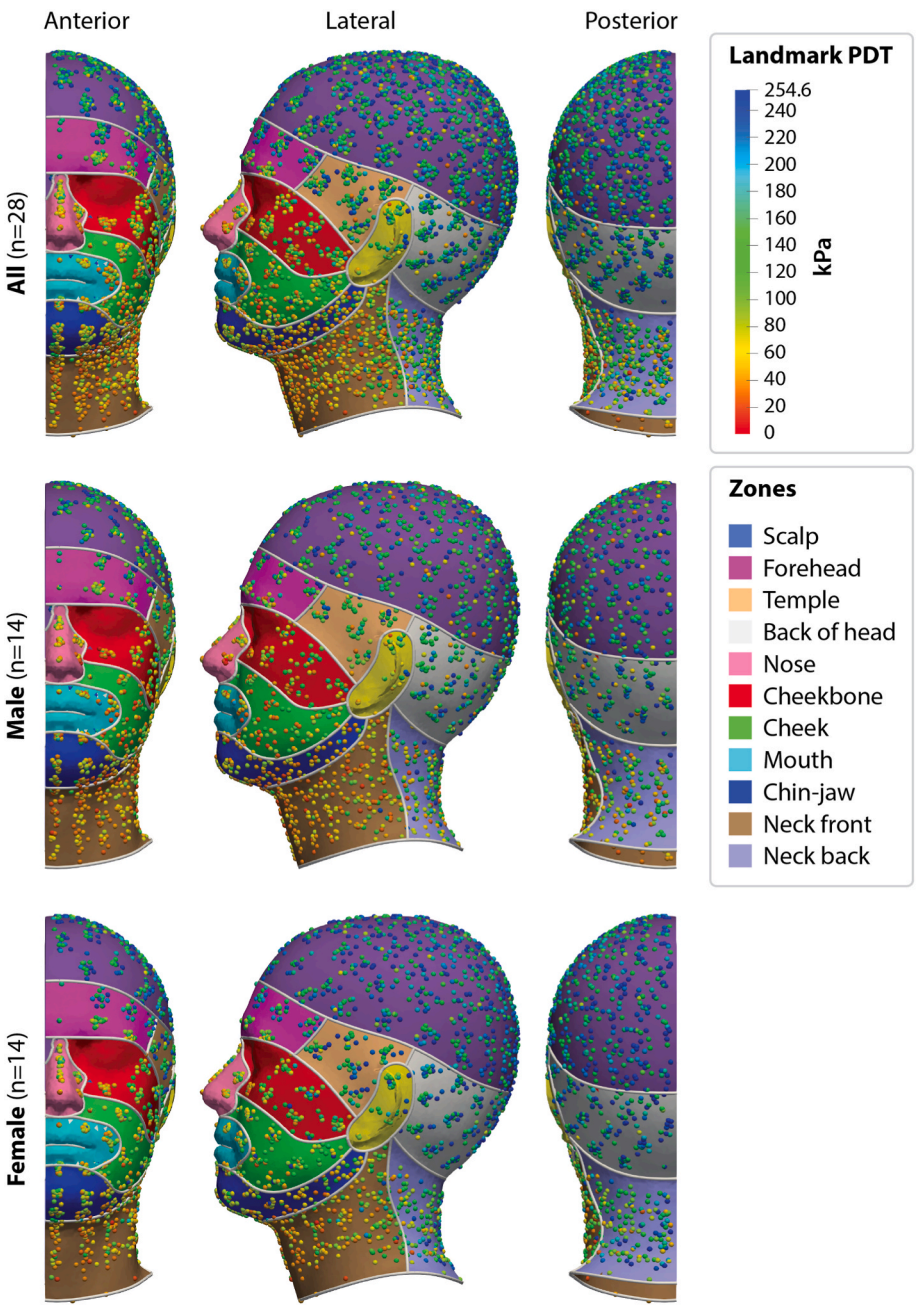


**Fig. 4.** PDT values in kPa per landmark within zones of all participants (n=28), males (n=14) and females (n=14), anterior, lateral and posterior view. Please note that shading is on to improve depth perception, which may affect colour (and thus PDT value) interpretation. The use of the digital model is advised (please see the *open data access* section). Please note that long hair of female participants and the pressure by the headcap may influence gender and zone differences (see also §4.2). (For interpretation of the references to colour in this figure legend, the reader is referred to the Web version of this article.)

### 3.2. PDT gender difference

Fig. 6 shows that females have a higher PDT than males. This is also true when looking at differences per zone (see Fig. 7 and Table 2). However, normalised PDT values (based on the Mean5%MaxPDT) of each landmark within each zone for males and females only significantly differ on the *scalp*, *back of the head* and *mouth* (see Fig. 8 and Table 2). This indicates that PDT is similarly distributed in males and females for the other zones.

### 3.3. PDT zone difference

As shown in Fig. 4 and Table 2, a low PDT was found in areas around the *nose*, *neck front*, *mouth*, *chin-jaw*, *cheek* and *cheekbone*. Medium PDT was found in the *neck back*, *forehead*, *temple*, and high PDT in the *back of the head* and *scalp*. The *scalp* and *back of the head*, *forehead* and *temple*, and the *nose*, *check bone*, *cheek*, *mouth*, *chin-jaw* and *neck front* provide (with a few exceptions) do not significantly differ. Arguably these zones could be treated as one zone (i.e. *parietal-occipital region*, *frontal-temporal region*, *face-front-neck region* respectively).

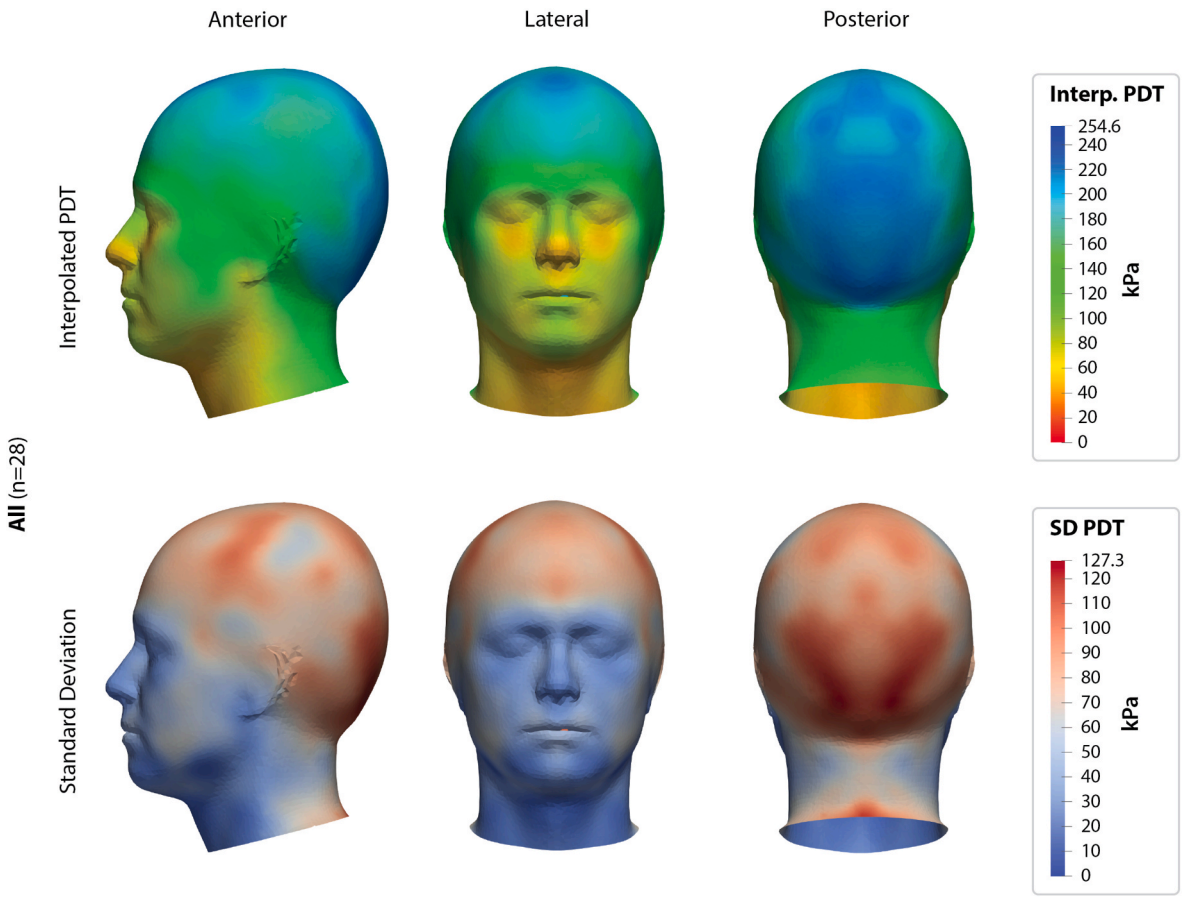


**Fig. 5.** Mean and SD interpolated PDT map in kPa of all participants (n=28), anterior, lateral and posterior view. Please note that shading is on to improve depth perception, which may affect colour (and thus PDT value) interpretation. The use of the digital model is advised (please see the *open data access* section). (For interpretation of the references to colour in this figure legend, the reader is referred to the Web version of this article.)

## 4. Discussion

The experiment results show that the *nose*, *neck front*, *mouth*, *chin-jaw*, *cheek* and *cheekbone* areas are most sensitive (low PDT), where the *neck back*, *forehead* and *temple* regions are medium-sensitive (medium PDT), and the *back of the head* and *scalp* are least sensitive (high PDT). This is in line with existing literature. Shah and Luximon (2021) found in Chinese adults (n=218), when investigating the entire head and parts of the neck, that the *facial region* was the most pressure sensitive area, where the *forehead* and *temporal region* where medium, and the *skull area* was least sensitive. Brough and Konz (1992) found in young adults (n=30), when investigating the top part of the head, the *temple area* to be the most sensitive, medium sensitive was the *inferior frontal area* and the *parietal region*, and least sensitive was the *superior frontal area* and *occipital region*. Broekhuizen et al. (2019) (n=19), who also investigated the top part of the head, fount the *inferior frontal area* to be most sensitive, medium sensitive in the *temple region*, *parietal eminence region*, *superior frontal* and *parietal region*, and least sensitive in the *superior occipital* and *inferior occipital region*.

When reanalysing the reported data by Broekhuizen et al. (2019) and Shah and Luximon (2021), by taking the mean of all landmarks within each zone as defined in this study, one can see a similar trend of pressure distribution on the head, face and neck (see Fig. 9). Noticeable is that Shah and Luximon (2021) pressure values are double of that of Broekhuizen et al. (2019) and this study. A possible explanation is the difference in probe used (Goonetilleke and Eng, 1994) or ethnicity of the tested populations (Komiyama et al., 2007). Where Broekhuizen et al. (2019) used a ø11.3 mm probe on a European population, Shah and Luximon (2021) used a ø3 mm on a Chinese population and this study ø10 mm on an International – but predominantly European – population.

Previous studies use fixed anatomical landmarks. This method allows for easier analysis, but limits landmark density (as clear anatomical landmarks are missing on undistinctive surfaces like the cheeks, forehead, scalp and neck, making accurate landmark placement difficult) and thereby model accuracy. This study introduces a new method, which allows for a dense landmark coverage without the need of anatomical landmarks. This method uses the 3D location of each landmark to make a comparison between participants and a PDT map by means of interpolation possible. The benefit of using 3D scanning to capture landmark locations is that it is more precise and allows for freedom of placement of landmarks.

The sparsity of anatomical landmarks in previous studies leads to a rough estimation of PDT in regions sparce of landmarks. The higher landmark density introduced in this study on head, face and neck PDT results in a more precise and detailed map. For example, comparing this study's results with that of Broekhuizen et al. (2019) and Shah and Luximon (2021) for the region above the eyebrows, shows that this study's PDT map is more accurately defined due to a denser probing of that area. Such finer PDT details could help designers and engineers to adjust their design to interface with less sensitive areas and spare sensitive areas.

### 4.1. Underlying tissue

The difference in PDT per area could be explained by the underlying tissue, such as skin thickness and underlying fat tissue, muscles, nerves, blood veins, cartilage, and bone. It could also be influenced by receptor

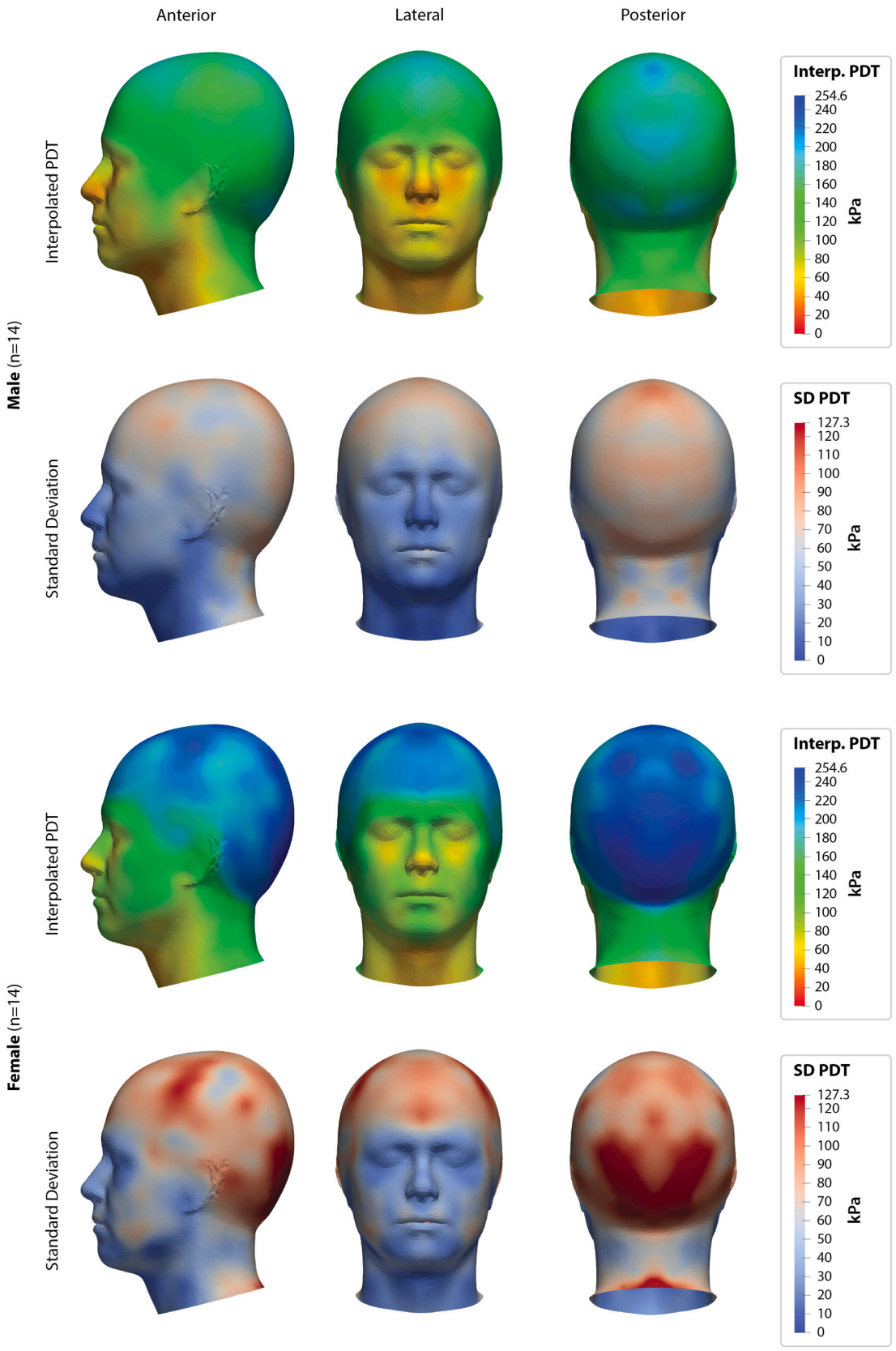


**Fig. 6.** Male and female mean and SD interpolated PDT map in kPa (n=14), anterior, lateral and posterior view. Please note that shading is on to improve depth perception, which may affect colour (and thus PDT value) interpretation. The use of the digital model is advised (please see the *open data access* section). Please note that long hair of female participant and the pressure by the headcap may influence gender and zone differences (see also §4.2). (For interpretation of the references to colour in this figure legend, the reader is referred to the Web version of this article.)

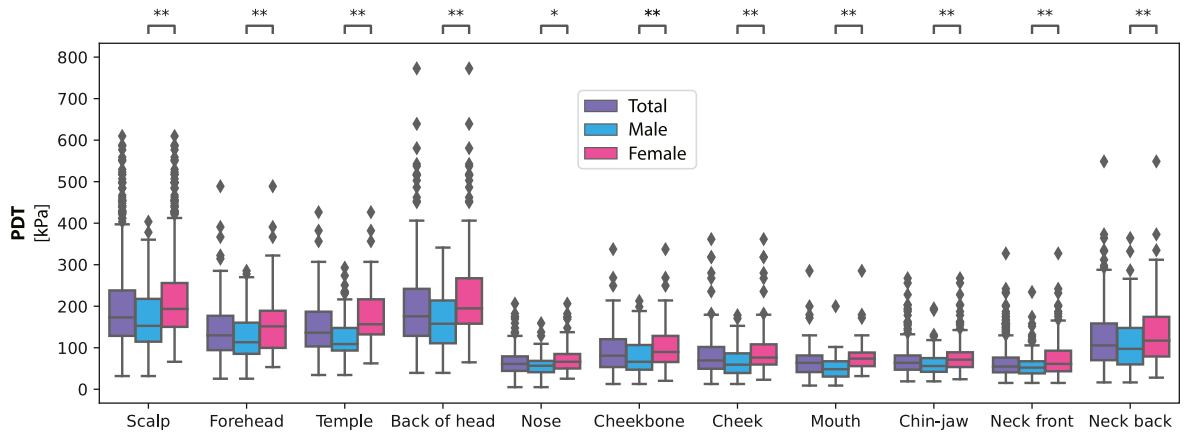


**Fig. 7.** PDT boxplot in kPa of all (n=28), male (n=14) and female (n=14) per zone. Sig.dif. between sexes per zone are indicated as *p≤0.05 and **p≤0.01. Please note that long hair of female participant and the pressure by the headcap may influence gender and zone differences (see also §4.2). (For interpretation of the references to colour in this figure legend, the reader is referred to the Web version of this article.)

**Table 2**
Mean (SD) measured PDT (in kPa) and normalised PDT of all (n=28), male (n=14) and female (n=14) and gender-based difference per zone per zone. Sig.dif. between sexes per zone are indicated as *p≤0.05 and **p≤0.01. Please note that long hair of female participant and the pressure by the headcap may influence gender and zone differences (see also §4.2).

| Zone | Measured PDT (in kPa) | | | | Normalised PDT (in percentage) | | | |
|---|---|---|---|---|---|---|---|---|
| | All mean (SD) (n=28) | Male mean (SD) (n=14) | Female mean (SD) (n=14) | Gender based difference *p-value* | All mean (SD) (n=28) | Male mean (SD) (n=14) | Female mean (SD) (n=14) | Gender based difference *p-value* |
| Scalp | 190.7 (83.8) | 167.3 (72.8) | 214.2 (94.9) | p≤0.01** | 74.8 (14.8) | 75.6 (15.0) | 74.1 (14.6) | p≤0.05* |
| Forehead | 144.1 (69.4) | 129.7 (62.9) | 158.6 (75.9) | p≤0.01** | 57.7 (18.7) | 58.7 (18.1) | 56.6 (19.4) | .42 |
| Temple | 151.2 (64.7) | 125.2 (56.5) | 177.3 (73) | p≤0.01** | 59.6 (14.0) | 57.7 (15.4) | 61.5 (12.4) | .09 |
| Back of head | 196.1 (91.7) | 165.4 (72.3) | 226.8 (111.1) | p≤0.01** | 74.5 (15.1) | 72.2 (15.4) | 77.0 (14.5) | p≤0.01** |
| Nose | 67.1 (34.2) | 59 (28.9) | 75.3 (39.6) | p≤0.05* | 27.5 (12.0) | 27.8 (12.0) | 27.3 (12.2) | .75 |
| Cheekbone | 92 (50.6) | 80 (45.4) | 104 (55.8) | p≤0.01** | 35.9 (13.4) | 35.8 (13.7) | 36.0 (13.2) | .96 |
| Cheek | 80.1 (47.9) | 66.5 (36.2) | 93.8 (59.7) | p≤0.01** | 30.5 (10.1) | 29.6 (10.7) | 31.4 (9.3) | .11 |
| Mouth | 67.3 (37.9) | 53.6 (32.9) | 81 (43) | p≤0.01** | 26.7 (10.9) | 24.5 (11.5) | 28.8 (10.0) | p≤0.01** |
| Jaw-chin | 70.3 (34.8) | 61.1 (27.8) | 79.5 (41.8) | p≤0.01** | 28.8 (10.9) | 30.2 (11.9) | 27.5 (9.7) | .11 |
| Neck front | 65 (35.8) | 56.1 (27.1) | 73.9 (44.6) | p≤0.01** | 26.4 (11.4) | 26.9 (11.6) | 25.8 (11.1) | .45 |
| Neck back | 121 (69.8) | 108.7 (64.5) | 133.3 (75.1) | p≤0.01** | 47.0 (17.4) | 48.3 (19.4) | 45.7 (15.1) | .26 |

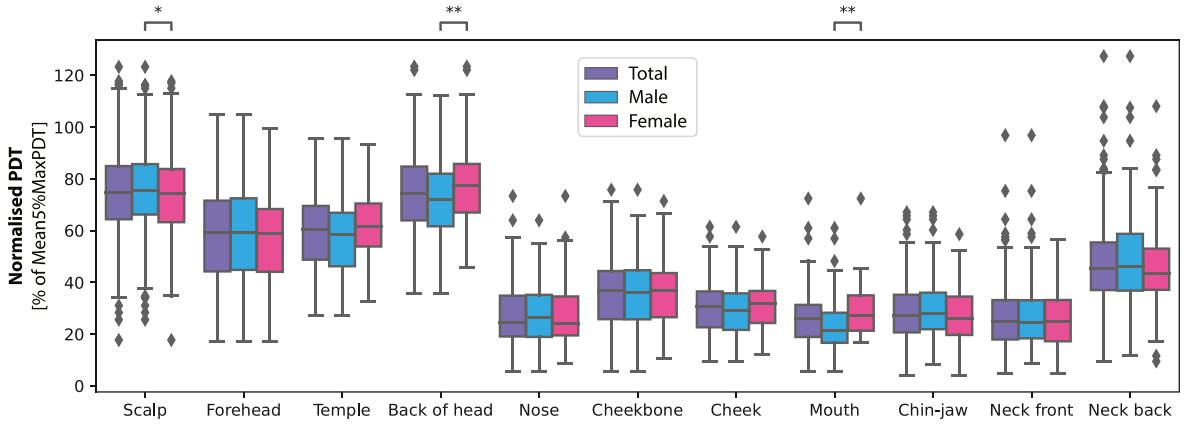


**Fig. 8.** Normalised PDT boxplot of all (n=28), male (n=14) and female (n=14) per zone. Sig.dif. between sexes per zone are indicated as *p≤0.05 and **p≤0.01. Please note that long hair of female participant and the pressure by the headcap may influence gender and zone differences (see also §4.2). (For interpretation of the references to colour in this figure legend, the reader is referred to the Web version of this article.)

density. For instance, in the cheek and nose receptors are more proximate to each other than in the forehead (Corniani and Saal, 2020). In areas with excess subcutaneous fat, people are less sensitive (Price et al., 2013). However, Shah and Luximon (2021) found that PDT of the head was independent of BMI.

That said, regions with a high density of receptors like the *nose* (*nasal region*) and area around the *mouth* (*oral region*) show a low PDT. As do areas with arteries like the *temple* and *front neck*, where the latter also contains critical soft tissue like the *trachea* and *oesophagus*. Also noticeable is the sensitivity around the eyes (*orbital region*), and especially above the eye at the eyebrows and lower part of the *forehead* (*inferior frontal region*). Possibly these zones are extra sensitive in order

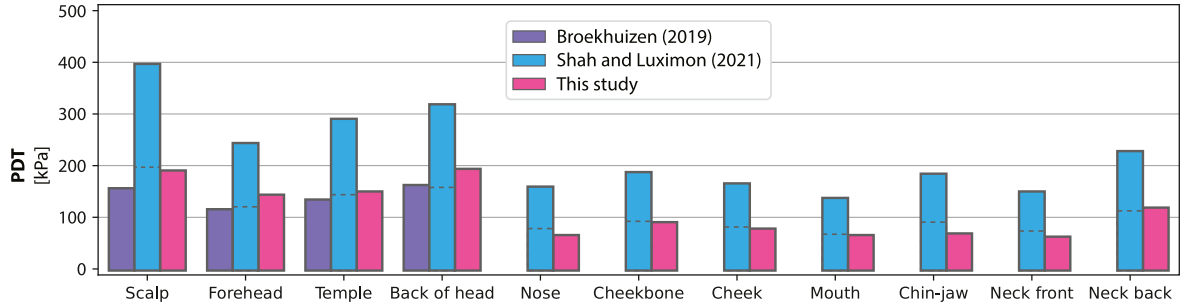


**Fig. 9.** Mean PDT per zone in kPa for Broekhuizen et al. (2019) (n=19), Shah and Luximon (2021) (n=218) and this study (n=28). (For interpretation of the references to colour in this figure legend, the reader is referred to the Web version of this article.)

to protect one of our most dominant and vulnerable sensors: the eyes. Tissue proximate to bone like the *cheekbone*, *chin* and *scalp* are less sensitive than their proximate regions with more underlying soft tissue. The big exception here is the *back of the neck*, possibly due to the high density of strong muscle tissue.

### 4.2. Differences between sexes

Fischer (1987) found that females had a lower PDT/PPT than men at the *lower* and *upper back* and *shoulders*. Antonaci et al. (1992) found no significant differences in PPT between sexes, where Jensen et al. (1992) also found that females had a lower PPT than men. Hung and Samman (2009) found a higher pain detection threshold in males, especially in the *chin* and the *right infraorbital areas*. Lee et al. (1994) found no definitive correlation between PPT and gender, but found that PPT in the *head* and *neck* muscles were generally lower in women than in men. Stefani et al. (2012) found a lower PPT in females at the *mid-forearm*, but gender influence was not statistically significant. Melia et al. (2019) found that men, as well as manual labourers, had comparatively higher adjusted PPT in the *forehead*, *temple*, *m. masseter* and *m. sternocleido-mastoid* than females. Broekhuizen et al. (2019) found that women had a lower PDT than males on the whole head (*frontal*, *parietal*, *temporal* and *occipital regions*). Shah and Luximon (2021) found that females had a lower PDT than males in two-third of their 76 landmarks on the head, face and neck.

Opposite to most literature, this study's results indicate that women are – based on absolute PDT values – less sensitive than men (higher PDT), especially on the scalp. Normalised PDT values (based on the Mean5%MaxPDT) of each landmark within each zone for males and females only significantly differ on the *scalp*, *back of the head* and *mouth*, indicating that PDT is similarly distributed in males and females for the other zones. This is an important insight, as it indicates no gender deviating product-human interface distribution is needed. However, gender difference in absolute pressure tolerance should possibly be considered in product-human interface design.

A possible explanation for the found absolute pressure difference could be that the female participants had long hair, which – although put in a knot to the side to minimise hair between cap and skin – could have damped and spread the applied pressure. E.g. the results of Myles et al. (2015) suggest that hair density might slightly impede vibration signals from reaching the scalp and reduce vibration sensitivity, for the least sensitive locations on the head. Also hair thickness (fine, medium and coarse) and type (straight, curly) could play a role, as suggested – but not investigated – by Brough and Konz (1992). Another explanation could be the constant pull of long hair to the skin, making these females used to a certain amount of (tension) force on their scalp skin, resulting in other PDT's.

### 4.3. Design implications

The use of a 3D head, face and neck PDT map could help designers and engineers create better and more comfortable products interfacing with the head, face and neck, e.g. by mounting equipment on and interface between human and product on less sensitive areas. Meanwhile, the PDT map can also contribute to the design of medical devices, e.g. as an indication to prevent medical device related pressure ulcers (Black et al., 2015; Gefen et al., 2020), and as a threshold of discomfort in applying diagnostics tools/physical interventions (Posnick et al., 1990).

Vink and Lips (2017) found low PDT in the buttocks, where Zenk et al. (2012) found that long term discomfort (>2h) was weaker in the buttocks than in the knee cavities. This suggests that PDT can indicate long term discomfort effects. Arguably, the present study results could thus be used for designing equipment which prolongedly interfaces with the head, face and neck. Keeping in mind that using a tool like this head, face and neck PDT map, always requires considered decision making by designers and engineers (Hiemstra-van Mastrigt et al., 2019).

However, long term contact – which can cause besides pressure also shear force, and isolation of heat and moisture/sweat – may lead to discomfort in the long run, or can even lead to rashes, swelling, ulcers or sores (Bhattacharya and Mishra, 2015; Gefen et al., 2020; Goossens, 2009; Goossens et al., 1994; Singh et al., 2020). This is of specific importance in e.g. medical contexts, where patient impaired sensory perception or impaired ability to communicate discomfort can lead to medical device related pressure ulcers (Black et al., 2015; Gefen et al., 2020).

To aid designers and engineers e.g. in CAD, the average PDT was mapped to a statistical shape model (SSM) of the human head, developed on the CAESAR 3D Anthropometric Database (Robinette et al., 2002) (see Fig. 10). While the PDT on different geometric heads is available, it is an approximation using the mean PDT data (n=28) and may not be as representative for the respective populations they are mapped upon. Future works could be directed toward collecting a larger dataset on PDT as well as 3D shapes of the head/neck and the associated parameters. Based on this dataset a 4D multimodality SSM can be built to approximate PDTs for individuals within the population, and to identify which variables (a.o. shape, soft tissue thickness, gender, culture, ethnicity, etc.), if any, can explain intersubject variability of PDT.

### 4.4. Limitations and suggestions for further research

The 3D PDT map of the head, face and neck only gives an indication of (dis)comfort (sensitivity), as shear force, cutting of (micro-vein) blood flow and moisture (e.g. sweat) obstruction by loads of head, face and neck related equipment are not investigated. The map is also based on an internationally mixed sample of n=28. Although the sample size is relative comparable to previous studies (e.g. Antonaci et al. (1992); Broekhuizen et al. (2019); Brough and Konz (1992)), a larger sample size like Shah and Luximon (2021) could result in a more representative PDT map.

Also investigation of to what extent the PDT maps are comparable between ethnicities could be considered, as Ball et al. (2010) showed a

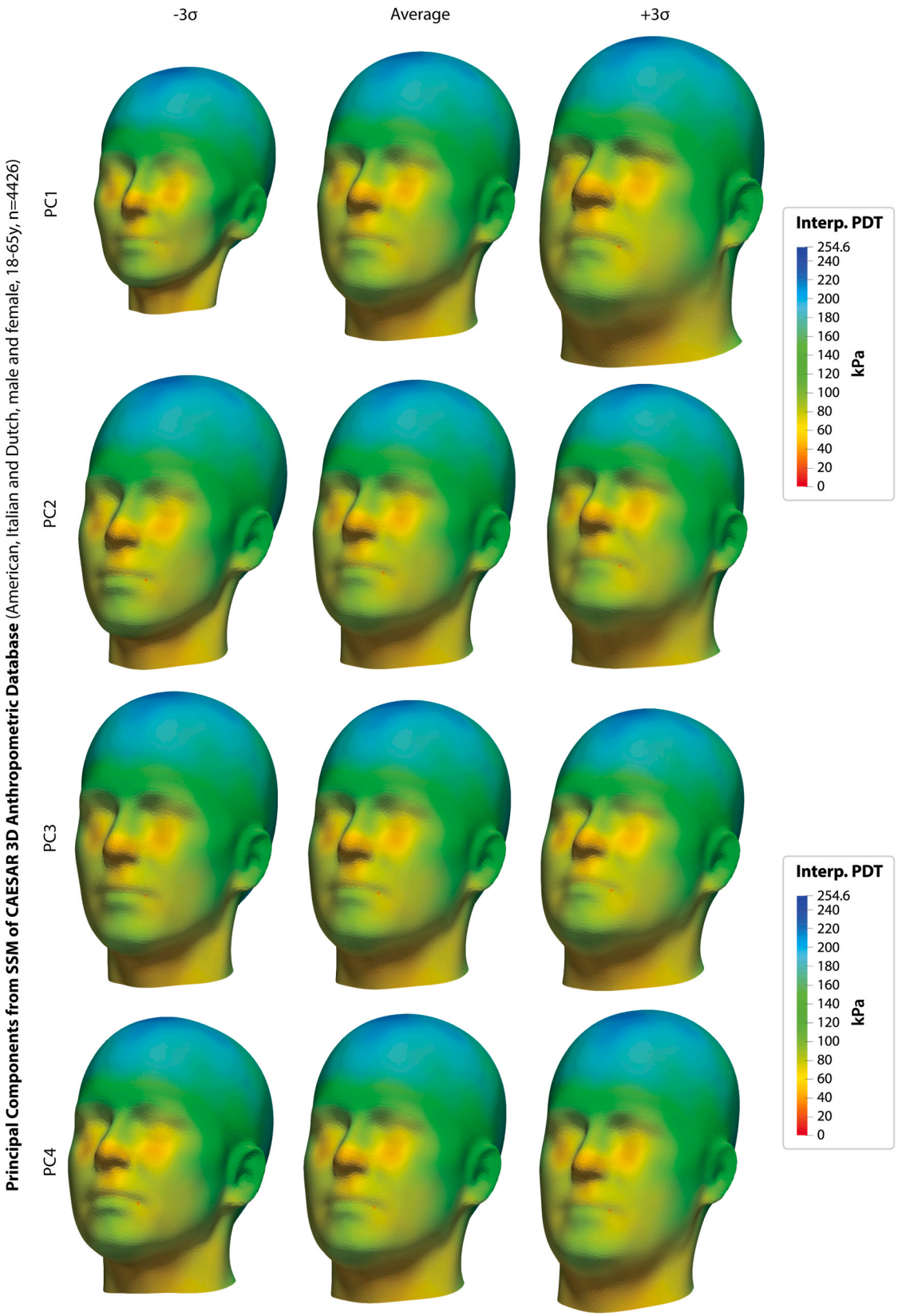


**Fig. 10.** Average PDT (based on n=28 sample from this study) mapped on the human head SSM (from Principal Component 1 to PC4, ±3σ) built on the CAESAR 3D Anthropometric Database (USA, Italy and The Netherlands, male and female, 18-65y, n=4309), isometric view. Please note that shading is on to improve depth perception, which may affect colour (and thus PDT value) interpretation. The use of the digital models is advised, which extends till PC50 (please see the *Open data access* section). (For interpretation of the references to colour in this figure legend, the reader is referred to the Web version of this article.)

significant difference in head shapes between Chinese and Caucasian, and Komiyama et al. (2007) found a difference in tactile and pain thresholds between Belgians and Japanese. Besides physical differences, cultural difference could influence (dis)comfort evaluations as well (Vink et al., 2021). When comparing Broekhuizen et al. (2019) and this study with Shah and Luximon (2021), difference can be seen (see Fig. 9), although probe size could of be influence here as well.

This study limits between-subject variability by means of normalisation based on the 5%MaxPDT, to limit the effect of outliers on the normalisation. That said, this normalisation method is based on subjective ratings. A maximal tolerated pressure test is more commonly used for normalisation (e.g. in EMG studies), but is not recommendable in a PDT study, as participants may go too far and exceed safe pressure limits. Normalisation based on a fixed pressure (e.g. 20, 50 and 80 kPa) on a fixed landmark (e.g. *philtrum*, *alare*, *sellion*, *tragion* and *glabella*) would not be a valid alternative, as it introduces another subjective scale. Future studies might consider physiological signals for objectification and normalisation of PDT (e.g. muscle contraction (EMG) or heartrate (ECG)).

Although this study has a high landmark density, the used landmark distance in this study (appr. 2–3 cm) can still be 'too big' to find subtle differences. Future work might want to investigate zones of interest in more detail, e.g. on and around the eyes, nose, ears and mouth for e.g. goggles, headphones and masks.

Although the landmarks were passed in a random order and successive stimulation of proximate landmarks were not noted, rare successive stimulation of adjacent landmarks without a sufficient interval might have influenced the PDT readings between them. For future studies, a randomiser which prevents successive stimulation of proximate landmarks is therefore recommended.

In addition, further research on the validity of short-term discomfort indication on actual experienced long-term comfort is needed, as is the evaluation of usability of the head, face and neck PDT map in product design. Also, the relation of PDT and underlying tissue could be investigated in more depth, e.g. from a medical, biomechanical and/or anatomical perspective.

In future research, capturing PDT data via an automated process (e.g. like Shah and Luximon (2021)) is advised, to save on time and staff.

## 5. Conclusion

A dense 3D pressure discomfort threshold (PDT) map of the human head, face and neck was made based on 126–146 left-lateral landmark locations in 28 participants (international, but majority European Caucasian, population). In comparison with previous studies, this study introduces a more landmark-dense, and therefore arguably a more detailed PDT map of the human head, face and neck. This study also introduces a new method where pressure discomfort threshold data is combined with 3D landmark locations, which are not limited to anatomically identifiable locations, allowing for more precision and freedom in placement of landmarks.

Results indicated that the *nose*, *neck front*, *mouth*, *chin-jaw*, *cheek* and *cheekbone* regions can tolerate the lowest pressure, where the *neck back*, *forehead* and *temple* regions are medium and the *back of the head* and *scalp* have the most tolerance, which is in line with existing literature.

This study also found that females have higher PDT levels than males in all regions, where most literature indicates the opposite. Further research on long-term pressure (dis)comfort and usability of this 3D PDT map are needed.

## Open data access

The 3D PDT maps (incl. PDT mapped on the SSM of the human head developed on the CAESAR 3D Anthropometric Database), average 3D head model and PDT data are available at data.4tu.nl (doi.org/10.4121/21482328) under CC BY-SA 4.0 licence. For privacy reasons, landmark coordinates and 3D scan mesh data of individual participants are not made available.

Please cite this publication when making use of the model and/or the data set. Users of the PDT maps are encouraged to share their experiences with the authors (e.g. via forum.dined.nl).

## Ethical approval

This study was approved by the Delft University of Technology *Human Research Ethical Committee* (hrec.tudelft.nl) on 18 July 2019 (approval no. 772), in accordance with The Helsinki Declaration (World Medical Association, 2013). Research materials and method, including a *'sticker allergic reaction test'*, were evaluated with a medical doctor and approved by a *Health, Safety and Environment Officer* of the Delft University of Technology.

Participants recognisable on pictures and 3D scans gave explicit permission to be recognisable in this publication. Other models are maps on a generic head model made of merging all 3D scans of all participants into one.

## Declaration of competing interest

This study was a collaboration between Crescent Medical B.V. and the Delft University of Technology in 2019-2020. Crescent Medical contributed to this study in manpower. Study set-up and execution were in collaboration with Crescent Medical, but Crescent Medical was not involved in, nor had influence on the analysis and creation of the 3D PDT maps. Crescent Medical had early access to the 3D PDT maps for designing a surgical headset, before making the maps accessible to the public in 2022.

## Acknowledgments

We want to thank miss L. Di Brigida and mr. B.J. Naagen for their assistance in conducting this study. We also want to thank E. Heesterbeek (MD) for medical safety consulting, and dr. T. Albin for his advice on statistics. Crescent Med, in particular ir. S.R. Andary, for supporting this study by making manhours available. This study was partly financed by the Dutch Research Council (NWO) (project number: 18636).

The authors would also like to acknowledge the previous unpublished work of our MSc. students on sensitivity of different features of the head for a multitude of design projects, as their work showed the need and laid the groundwork for a full head PDT model: B. Bossenbroek, J. van Dijk, L. Kok, T. Paclik, J. Snoek, G. van Soelen; T.A. Rotte, M. Otten, Z.M. Hayde, V. Aus dem Kamen, P. Mösinger, J.E. Sanchez; S. Krabbenborg, A. Bisnajak, A. Abarca, E. Liermann, P. Bosch and N. van den Brink.

And last but not least all the volunteers who were so kind to take part in this study.

## References

Antonaci, F., Bovim, G., Fasano, M., Bonamico, L., Shen, J., 1992. Pain threshold in humans. A study with the pressure algometer. Funct. Neurol. 7 (4), 283–288.

Ball, R., Shu, C., Xi, P., Rioux, M., Luximon, Y., Molenbroek, J.F.M., 2010. A comparison between Chinese and Caucasian head shapes. Appl. Ergon. 41 (6), 832–839. https://doi.org/10.1016/j.apergo.2010.02.002.

Bhattacharya, S., Mishra, R., 2015. Pressure ulcers: current understanding and newer modalities of treatment. Indian J. Plast. Surg. 48 (01), 004–016. https://doi.org/10.4103/0970-0358.155260.

Black, J., Alves, P., Brindle, C.T., Dealey, C., Santamaria, N., Call, E., Clark, M., 2015. Use of wound dressings to enhance prevention of pressure ulcers caused by medical devices. Int. Wound J. 12 (3), 322–327. https://doi.org/10.1111/iwj.12111.

Broekhuizen, R., De Rydt, T., Lutters, E., Ten Klooster, R., De Bruyne, G., 2019. Head sensitivity for designing bicycle helmets with improved physical comfort. In: Rebelo, F., Soares, M. (Eds.), Advances in Ergonomics in Design. AHFE 2018. Advances in Intelligent Systems and Computing, 777. Springer, Cham, Switzerland, pp. 14–19. https://doi.org/10.1007/978-3-319-94706-8_2.

Brough, P., Konz, S., 1992. Pressure sensitivity of the head. In: Kumar, S. (Ed.), Advances in Industrial Ergonomics and Safety IV. Taylor & Francis, London, UK, pp. 633–636. https://doi.org/10.1201/9781482272383.
Buso, A., Shitoot, N., 2019. Sensitivity of the foot in the flat and toe off positions. Appl. Ergon. 76, 57–63. https://doi.org/10.1016/j.apergo.2018.12.001.
Corniani, G., Saal, H.P., 2020. Tactile innervation densities across the whole body. J. Neurophysiol. 124 (4), 1229–1240. https://doi.org/10.1152/jn.00313.2020.
Dyke, R.M., Lai, Y.-K., Rosin, P.L., Zappalà, S., Dykes, S., Guo, D., Yang, J., 2020. SHREC'20: shape correspondence with non-isometric deformations. Comput. & Graph. 92, 28–43. https://doi.org/10.1016/j.cag.2020.08.008.
Fenko, A., Schifferstein, H.N., Hekkert, P., 2010. Shifts in sensory dominance between various stages of user–product interactions. Appl. Ergon. 41 (1), 34–40. https://doi.org/10.1016/j.apergo.2009.03.007.
Fischer, A.A., 1986. Pressure threshold meter: its use for quantification of tender spots. Arch. Phys. Med. Rehabil. 67 (11), 836–838.
Fischer, A.A., 1987. Pressure algometry over normal muscles. Standard values, validity and reproducibility of pressure threshold. Pain 30 (1), 115–126. https://doi.org/10.1016/0304-3959(87)90089-3.
Fransson-Hall, C., Kilbom, Å., 1993. Sensitivity of the hand to surface pressure. Appl. Ergon. 24 (3), 181–189. https://doi.org/10.1016/0003-6870(93)90006-u.
Franz, M., Durt, A., Zenk, R., Desmet, P., 2012. Comfort effects of a new car headrest with neck support. Appl. Ergon. 43 (2), 336–343. https://doi.org/10.1016/j.apergo.2011.06.009.
Gefen, A., Alves, P., Ciprandi, G., Coyer, F., Milne, C.T., Ousey, K., Worsley, P., 2020. Device-related pressure ulcers: SECURE prevention. J. Wound Care 29 (Suppl. 2a), S1–S52. https://doi.org/10.12968/jowc.2020.29.5.245.
Goonetilleke, R.S., Eng, T.J., 1994. Contact area effects on discomfort. In: Proceedings of the Human Factors and Ergonomics Society Annual Meeting, , 10th38. SAGE, Los Angeles, CA, USA, pp. 688–690. https://doi.org/10.1177/154193129403801032.
Goossens, R.H.M., 2009. Fundamentals of pressure, shear and friction and their effects on the human body at supported postures. In: Gefen, A. (Ed.), Bioengineering Research of Chronic Wounds. Studies in Mechanobiology, Tissue Engineering and Biomaterials, 1. Springer, Berlin, Heidelberg, pp. 1–30. https://doi.org/10.1007/978-3-642-00534-3_1.
Goossens, R.H.M., Zegers, R., van Dijke, G.H., Snijders, C., 1994. Influence of shear on skin oxygen tension. Clin. Physiol. 14 (1), 111–118. https://doi.org/10.1111/j.1475-097x.1994.tb00495.x.
Gower, J.C., 1975. Generalized procrustes analysis. Psychometrika 40 (1), 33–51. https://doi.org/10.1007/BF02291478.
Hiemstra-van Mastrigt, S., Smulders, M., Bouwens, J.M., Vink, P., 2019. Designing aircraft seats to fit the human body contour. In: Scataglini, S., Paul, G. (Eds.), DHM and Posturography. Elsevier, pp. 781–789. https://doi.org/10.1016/B978-0-12-816713-7.00061-1.
Hung, J., Samman, N., 2009. Facial skin sensibility in a young healthy Chinese population. Oral Surg. Oral Med. Oral Pathol. Oral Radiol. Endod. 107 (6), 776–781. https://doi.org/10.1016/j.tripleo.2008.10.026.
Huysmans, T., Goto, L., Molenbroek, J.F.M., Goossens, R.H.M., 2020. DINED mannequin. Tijdschrift voor Human Factors 45 (1), 4–7.. Retrieved from. https://www.humanfactors.nl/tijdschrift/download/nummer-1-april-2020/176.
Jasper, H.H., 1958. Report of the committee on methods of clinical examination in electroencephalography. Electroencephalogr. Clin. Neurophysiol. 10 (2), 370–375. https://doi.org/10.1016/0013-4694(58)90053-1.
Jensen, R., Rasmussen, B.K., Pedersen, B., Lous, I., Olesen, J., 1992. Cephalic muscle tenderness and pressure pain threshold in a general population. Pain 48 (2), 197–203. https://doi.org/10.1016/0304-3959(92)90059-k.
Komiyama, O., Kawara, M., De Laat, A., 2007. Ethnic differences regarding tactile and pain thresholds in the trigeminal region. J. Pain 8 (4), 363–369. https://doi.org/10.1016/j.jpain.2006.12.002.
Lee, K.H., Lee, M.H., Kim, H.S., Kim, J.H., Chung, S.C., 1994. Pressure pain thresholds [PPT] of head and neck muscles in a normal population. J. Muscoskel. Pain 2 (4), 67–81. https://doi.org/10.1300/j094v02n04_06.
Lee, W., Kim, J.G., Molenbroek, J.F.M., Goossens, R.H.M., You, H., 2019. Estimation of facial contact pressure based on finite element analysis. In: Di Nicolantonio, M., Rossi, E., Alexander, T. (Eds.), Advances in Additive Manufacturing, Modeling Systems and 3D Prototyping. AHFE 2019. Advances in Intelligent Systems and Computing, 975. Springer. Cham, Switzerland. https://doi.org/10.1007/978-3-030-20216-3_61.
Melia, M., Geissler, B., König, J., Ottersbach, H.J., Umbreit, M., Letzel, S., Muttray, A., 2019. Pressure pain thresholds: subject factors and the meaning of peak pressures. Eur. J. Pain 23 (1), 167–182. https://doi.org/10.1002/ejp.1298.
Mergl, C., 2006. Entwicklung eines verfahrens zur optimierung des sitzkomforts auf Automobilsitzen. Technische Universität München, München, Germany.. Retrieved from. http://mediatum.ub.tum.de/?id=601975
Myles, K., Kalb, J.T., Lowery, J., Kattel, B.P., 2015. The effect of hair density on the coupling between the tactor and the skin of the human head. Appl. Ergon. 48, 177–185. https://doi.org/10.1016/j.apergo.2014.11.007.
O'Hora, L., Robbins, E., Savidge, L., Tokarick, B., Wood, B., Holbein-Jenny, M.A.. Pain pressure threshold (PPT). . Retrieved from. www.apta.org/patient-care/evidence-based-practice-resources/test-measures/pain-pressure-threshold-ppt.
Oostendorp, T.F., van Oosterom, A., Huiskamp, G., 1989. Interpolation on a triangulated 3D surface. J. Comput. Phys. 80 (2), 331–343. https://doi.org/10.1016/0021-9991(89)90103-4.
Parsons, K., 2003. Human Thermal Environments: the Effects of Hot, Moderate, and Cold Environments on Human Health, Comfort and Performance. CRC press, London, UK. https://doi.org/10.1201/9781420025248.
Posnick, J.C., Zimbler, A.G., Grossman, J., 1990. Normal cutaneous sensibility of the face. Plast. Reconstr. Surg. 86 (3), 429–433. https://doi.org/10.1097/00006534-199009000-00006.
Price, R., Asenjo, J., Christou, N., Backman, S., Schweinhardt, P., 2013. The role of excess subcutaneous fat in pain and sensory sensitivity in obesity. Eur. J. Pain 17 (9), 1316–1326. https://doi.org/10.1002/j.1532-2149.2013.00315.x.
Ramot, Y., Haim-Zada, M., Domb, A.J., Nyska, A., 2016. Biocompatibility and safety of PLA and its copolymers. Adv. Drug Deliv. Rev. 107, 153–162. https://doi.org/10.1016/j.addr.2016.03.012.
Robinette, K.M., Blackwell, S., Daanen, H., Boehmer, M., Fleming, S., 2002. Civilian American and European Surface Anthropometry Resource (Caesar), Final Report, Volume 1: Summary. United States Air Force Research Laboratory, Ohio, USA.. Retrieved from. https://www.humanics-es.com/CAESARvol1.pdf
Shah, P.B., Luximon, Y., 2021. Assessment of pressure sensitivity in the head region for Chinese adults. Appl. Ergon. 97, 103548 https://doi.org/10.1016/j.apergo.2021.103548.
Shah, P.B., Luximon, Y., Luximon, A., 2017. Use of soft tissue properties for ergonomic product design. In: Goonetilleke, R., Karwowski, W. (Eds.), Advances in Physical Ergonomics and Human Factors. AHFE 2017. Advances in Intelligent Systems and Computing, 602. Springer, Cham, Switzerland. https://doi.org/10.1007/978-3-319-60825-9_19.
Singh, M., Pawar, M., Bothra, A., Maheshwari, A., Dubey, V., Tiwari, A., Kelati, A., 2020. Personal protective equipment induced facial dermatoses in healthcare workers managing Coronavirus disease 2019. J. Eur. Acad. Dermatol. Venereol. 34, e378–e380. https://doi.org/10.1111/jdv.16628.
Stefani, L.C., da Silva Torres, I.L., De Souza, I.C.C., Rozisky, J.R., Fregni, F., Caumo, W., 2012. BDNF as an effect modifier for gender effects on pain thresholds in healthy subjects. Neurosci. Lett. 514 (1), 62–66. https://doi.org/10.1016/j.neulet.2012.02.057.
Vink, P., Anjani, S., Udomboonyanupap, S., Torkashvand, G., Albin, T., Miguez, S., Vanacore, A., 2021. Differences and similarities in comfort and discomfort experience in nine countries in Asia, the Americas and Europe. Ergonomics 64 (5), 553–570. https://doi.org/10.1080/00140139.2020.1853248.
Vink, P., Hallbeck, S., 2012. Editorial: comfort and discomfort studies demonstrate the need for a new model. Appl. Ergon. 43 (2), 271–276. https://doi.org/10.1016/j.apergo.2011.06.001.
Vink, P., Lips, D., 2017. Sensitivity of the human back and buttocks: the missing link in comfort seat design. Appl. Ergon. 58, 287–292. https://doi.org/10.1016/j.apergo.2016.07.004.
World Medical Association, 2013. World medical association declaration of Helsinki: ethical principles for medical research involving human subjects. JAMA 310 (20), 2191–2194. https://doi.org/10.1001/jama.2013.281053.
Xiong, S., Goonetilleke, R.S., Jiang, Z., 2011. Pressure thresholds of the human foot: measurement reliability and effects of stimulus characteristics. Ergonomics 54 (3), 282–293. https://doi.org/10.1080/00140139.2011.552736.
Zenk, R., Franz, M., Bubb, H., Vink, P., 2012. Spine loading in automotive seating. Appl. Ergon. 43 (2), 290–295. https://doi.org/10.1016/j.apergo.2011.06.004.
Zenk, R., Mergl, C., Hartung, J., Sabbah, O., Bubb, H., 2006. Objectifying the comfort of car seats. SAE Technical Paper, 2006-01-1299. https://doi.org/10.4271/2006-01-1299.
Zhuang, Z., Bradtmiller, B., 2005. Head-and-face anthropometric survey of U.S. respirator users. J. Occup. Environ. Hyg. 2 (11), 567–576. https://doi.org/10.1080/15459620500324727.